Evolution in Electrical and Electronic Engineering Vol. 4 No. 2 (2023) 258-266

EEEE

Homepage: http://publisher.uthm.edu.my/periodicals/index.php/eeee
e-ISSN : 2756-8458

Modelling and Analysis of Outdoor Composite Insulators Under Different Pollution Conditions

Muhammad Syafiq Kasmazuli[1], Rahisham Abd Rahman[1]*, Rizwan[1], Ali Salem[1]

[1]Faculty of Electrical and Electronic Engineering,
Universiti Tun Hussein Onn Malaysia, 86400 Parit Raja, Batu Pahat, Johor, MALAYSIA

*Corresponding Author Designation

DOI: https://doi.org/10.30880/eeee.2023.04.02.033
Received 27 June 2023; Accepted 15 August 2023; Available online 30 October 2023

Abstract: This paper presents modelling and analysis of the electric potential and electric field of a 33kV outdoor composite insulator. While composite insulators offer benefits like hydrophobicity, lightweight, and low maintenance, they are susceptible to stress and pollutants, compromising their efficiency and leading to flashovers. The model of the insulator is developed using COMSOL Multiphysics FEA software to simulate and determine the electric potential and electric field variation across the insulator under different pollution conditions. Bird dropping, Silica sand, Salt and Dust layers were used as the variable pollution. The simulation shows the electric potential decreased by 0.452% and the electric field increased by 3.53% while in humid conditions. Meanwhile among all the polluted conditions, Silica Sand gains the highest electric potential in humid and non-humid conditions by 1.39% and 1.30% of different percentages. The highest electrical field gain in humid and non-humid was Silica Sand and Bird dropping by 83.34% and 5.03%. The graph electric potential plot shows a decrement along the insulator length. The electric field graph plots maximum values at terminal high voltage and grounding while the minimum value plots at the shed's insulator. The increment of the polluted layer thickness increased the electric field line by 1.97% and decreased the electric potential by 0.83037%. Thus, the type of polluted conditions significantly affects the electric field and electric potential performance.

Keywords: Outdoor Composite Insulators**,** COMSOL Multiphysics FEA

1. Introduction

Composite insulators are well-known as good electrical insulation and suitable products for high-voltage usage in substations, distribution, and transmission lines. It has many advantages such as good hydrophobic nature, lightweight, low installation cost, easy handling and low maintenance [1]. It consists of three main parts which are the core, housing, and end connection. The housing is usually made from silicone rubber coating with a high hydrophobicity property. It prevents water from

Corresponding author: rahisham@uthm.edu.my

spreading across their surface to lower the leakage current [2]. The core and end connections are made from FRP and metal. However, insulators may be exposed to many types of stress and pollutants like bird dropping, acid rain and lightning strikes [3] This pollution condition makes the insulator brittle or break and lose its efficiency [1]. This condition can lead to surface heating, dry band formation and flashover. [4].

This project aims to analyse clean insulators in humid and non-humid conditions. Besides, to compare variations in the electric field under polluted and clean environmental conditions. Other than that, to study the effect of pollution layer thickness on the performance of composite insulators. This project will analyse the electric potential and electric field for insulators under various polluted conditions with humid and non-humid.

2. Methodology

The materials and methods section, otherwise known as methodology, describes all the necessary information that is required to obtain the results of the study.

2.1 Flowchart of the work progress

Figure 1 shows the flowchart of the work progress for the modelling and analysis of composite insulators under different pollution conditions. This figure has accomplished three objectives which are stated as (i) for objective 1, (ii) for objective 2 and (iii) for objective 3.

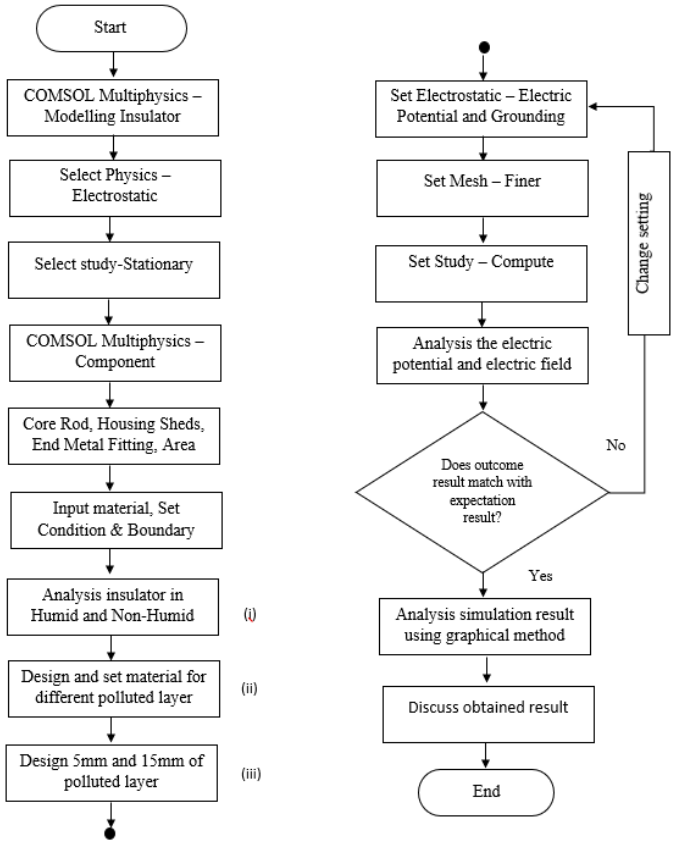

Figure 1: The flowchart of the work progress

2.2 Modelling and Simulation of Outdoor Composite Insulator

Table 1 presents the technical specifications of the insulator utilized in the simulation. The specifications were obtained from the model described in [5] and were used for the analysis.

Table 1: Technical specifications of insulator used in simulation [5],[6]

Type	Suspension insulator
Rated voltage (kV)	33
Rated mechanical load (kN)	70
Shed arrangement type	Uniform shed
Creepage distance (mm)	430
Arcing distance (mm)	180
Sectional length (mm)	360
Core thickness (mm)	18
No. of sheds	4
Shed Diameter (mm)	85
Shed Spacing (mm)	35
Metal End Fitting type	Socket fittings

Figure 2 shows the dimension geometry of the outdoor composite insulator launched by the 2D axisymmetric in the COMSOL Software. The modelled were specified at the millimetre scale for accurate representation and computational efficiency. The component of the insulator must be modelled first before running the simulation. The sheds, end metal fitting and core insulator were designed specifically based on [5] and [6]. The boundary conditions, material properties and mesh can be implemented if this geometric modelling is complete.

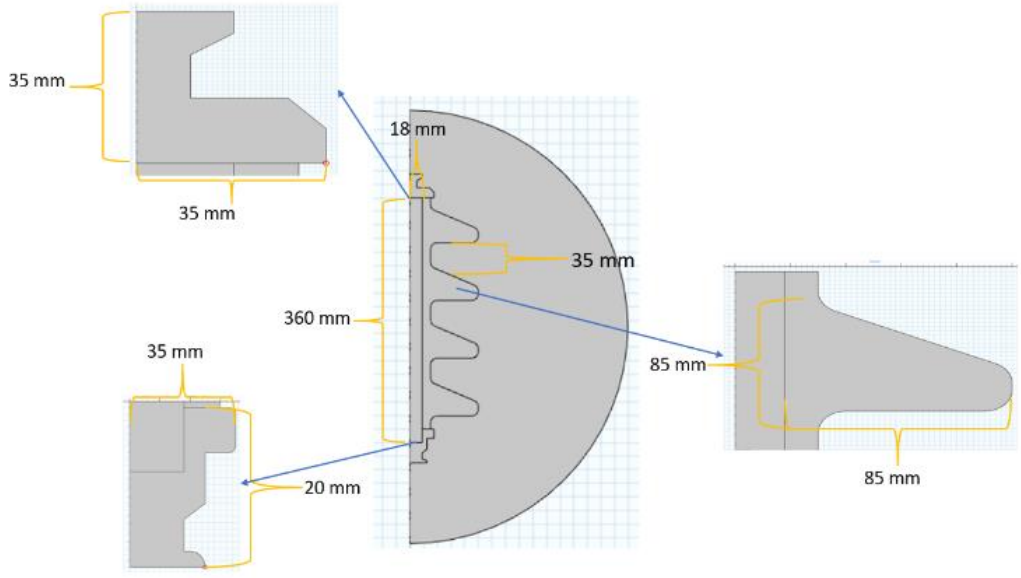

Figure 2: Dimension of 33 kV outdoor composite insulator

Figure 2 shows the relative permittivity and conductivity of material for the outdoor composite insulator. The material was set inside the modelled region after there was no overlap in the geometry design.

Table 2: Relative permittivity and conductivity for composite insulator

Material	Relative permittivity, ε_r	Conductivity, $\sigma\ (S/m)$
Forged steel (end fittings)	1	5.9×10^{7}
FRP (core)	7.2	1.0×10^{-12}
Silicone rubber (sheds)	4.3	1.0×10^{-12}
Air background	1	1.0×10^{-13}
Water Droplets	80	1.0×10^{-13}

2.3 Analysis of clean insulator under humid and non-humid conditions

To achieve objective 1, Figure 3 was modelled to adequately fill the top of insulator sheds. Four hemispherical water droplets with a contact angle of 90◦ represent a humid condition [7].

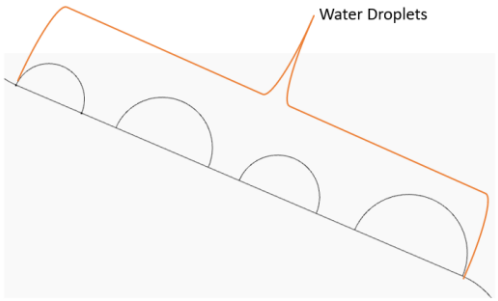

Figure 3: The water droplets on the insulator shed.

2.4 Compare the variation in electric field lines between clean and contaminated insulators.

To achieve objective 2, Figure 4 were modelled to compare the variation of the electric field under various condition.

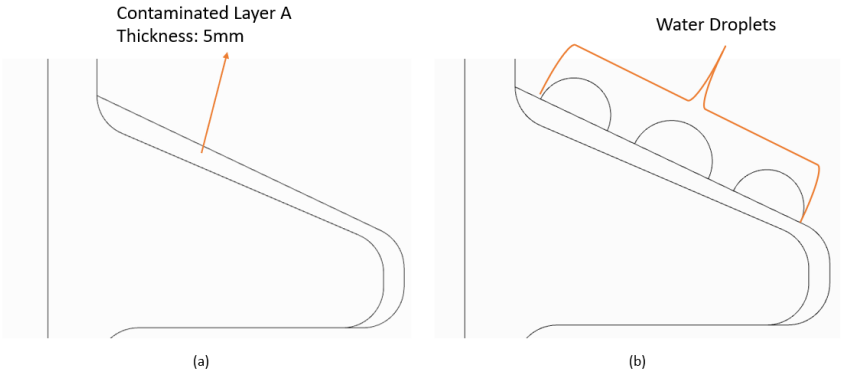

Figure 4: (a) Polluted Layer in Non-Humid, (b) Polluted Layer in Humid

Table 3 specifies the relative permittivity and conductivity of material-polluted layers. These materials were chosen due to their direct influence on the electric field performance.

Table 3: Relative permittivity and conductivity for the type of polluted layers

Material	Relative permittivity, ε_r	Conductivity, $\sigma\ (S/m)$	Reference
Bird dropping	20	1	[8]
Silica sand	3.5	5.0×10^{-10}	[9] [10]
Salt (NaCLO3)	5.7	5.0×10^{-7}	[11]
Dust Layer	10	30.0×10^{-9}	[12]

2.5 Study the influence of varied levels of pollution layer thickness on electric field lines

To achieve objective 3, Figure 5 was modelled to facilitate the analysis of the electric field. The model incorporated a 200% increment of thickness level and was tested using bird dropping as the contaminant material.

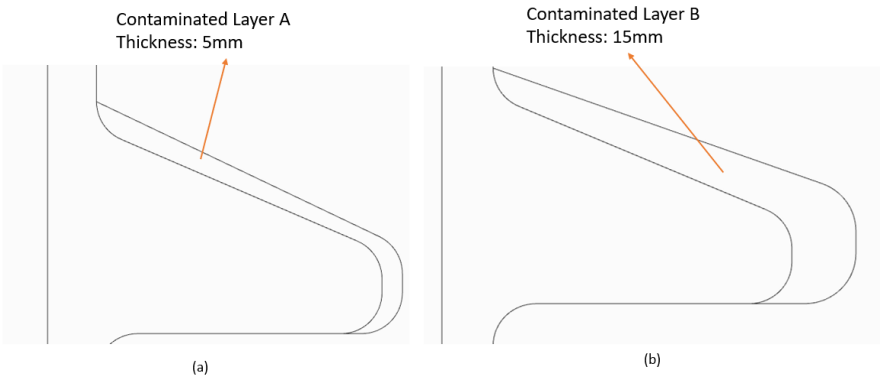

Figure 5: (a) Polluted Layer of 5mm (b) Polluted Layer of 15 m

3. Results and Discussion

3.1 Electric field distribution around clean insulators under humid and non-humid conditions

Figure 6 display a non-uniform electric field distribution line of 2D cutline across insulator for clean insulator in humid and non-humid condition. The humid insulator has a higher amplitude of electric field compared to the non-humid insulator. The x-axis in the range from 100mm to 300 mm represents the insulator shed area while the other is the end fitting. The circle labelled indicate the maximum and minimum point of the electric field for each condition. The non-humid insulator gained at 144300 V/m of the maximum electric field while the humid insulator gained at 149400 V/m. There is a 3.53% increment of the electric field in the presence of water droplets. This is because water's conductive properties attract electric field lines, creating areas of high field strength and increasing the risk of breakdown. Water droplets also have capacitance, storing electrical energy and affecting field strength and interactions with nearby objects.

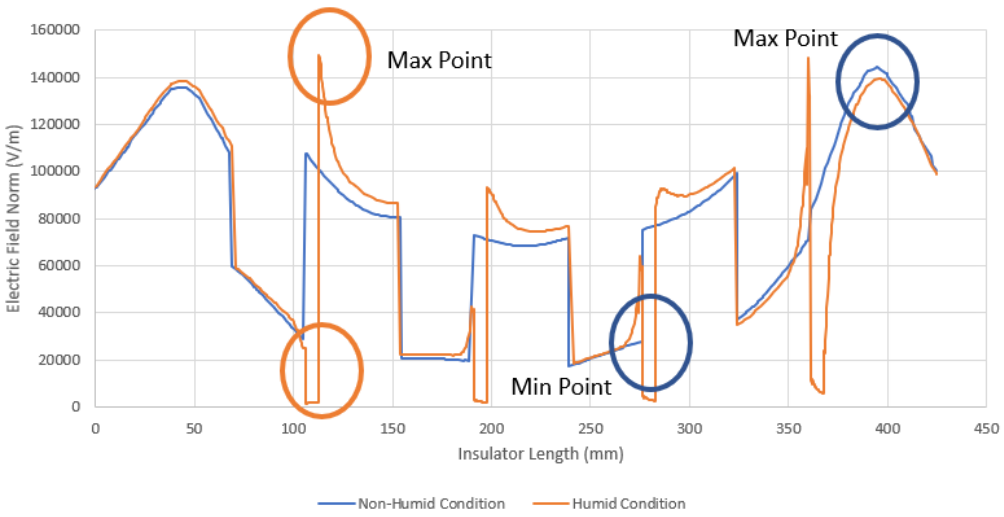

Figure 6: Electric field distribution in cross section 2D through a clean insulator (c) Non-Humid (d) Humid

3.2 Evaluation of electric field distribution for clean and contaminated insulator

Figure 7 depicts the graph of the electric field distribution line through various contaminated layers on an insulator in non-humid conditions. From the graph, the bird dropping gained the highest maximum electric field value with 14715 V/m. Then it was followed by a dust layer with 143600 V/m, Salt with 141300 V/m and Silica Sand with 140100 V/m. The values show that bird dropping has 5.03% different percentages compared with the Silica Sand. Thus, the bird dropping may have a higher dielectric constant compared to silica sand which allows it to store energy in the electric field, resulting in achieving the highest maximum electric field values.

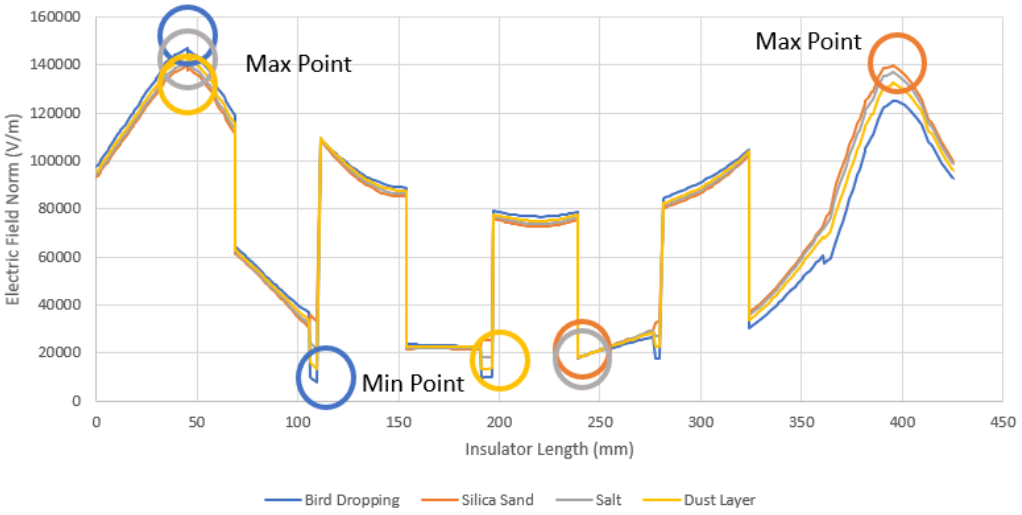

Figure 7: Electric field distribution in cross section 2D through a contaminated insulator (a) Bird Dropping (b) Silica Sand (c) Salt (NaCLO3) (d) Dust Layer in non-humid condition

Figure 7 depicts the graph of the electric field distribution line through various contaminated layers on the insulator in humid conditions. From the graph, the silica sand gained the highest maximum electric field value with 253800 V/m. Then it was followed by salt with 229200 V/m, dust layer with 195100 V/m and bird dropping with 152400 V/m. The values show that silica sand has an 83.34%

different percentage compared with the bird dropping. Water is a conductive material, and when it comes into contact with the silica sand it increases the conductivity and allows for a higher flow of electric current, resulting in a higher electric field strength. Meanwhile the conductivity of bird droppings remains relatively low compared to the other even the presence of water droplets. Thus, the bird droppings exhibit a minimal change in the electric field under humid conditions.

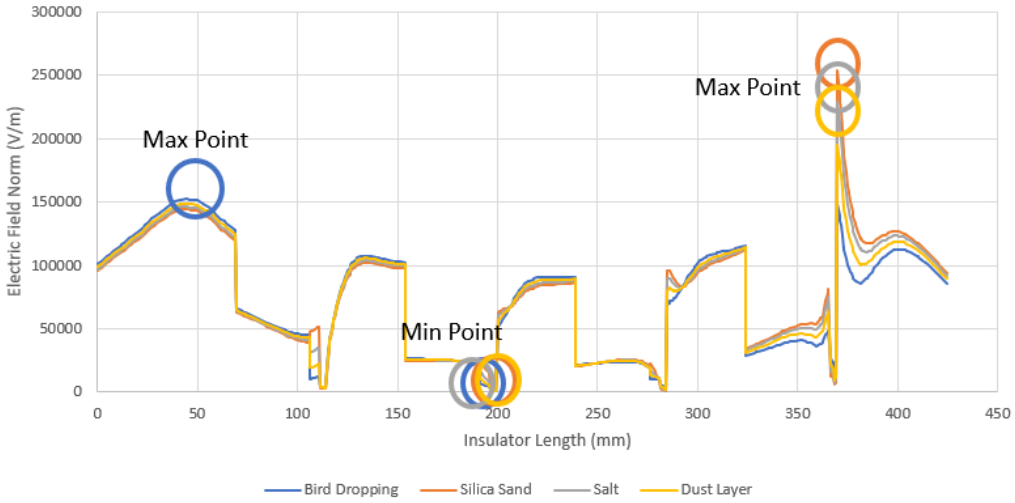

Figure 7: Electric field distribution in cross section 2D through a contaminated insulator (a) Bird Dropping (b) Silica Sand (c) Salt (NaCLO3) (d) Dust Layer in humid condition

Figure 8 depicts the graph of the electric field distribution line through bird-dropping contaminated layers on insulators in humid and non-humid conditions. From the graph, the bird-dropping in humid gained the highest maximum electric field value with 152400 V/m. Then it was followed by bird-dropping in non-humid with 147150 V/m and clean insulator in non-humid with 144300 V/m. The values show that both bird-dropping in humid and non-humid conditions have an increment percentage of difference maximum electric field by 5.62% and 1.97% compared with clean insulator in non-humid. The data shows the contaminated and water droplets can result in electrolytic effect. This electrolytic activity increases the conductivity of the bird droppings, also leading to a higher electric field.

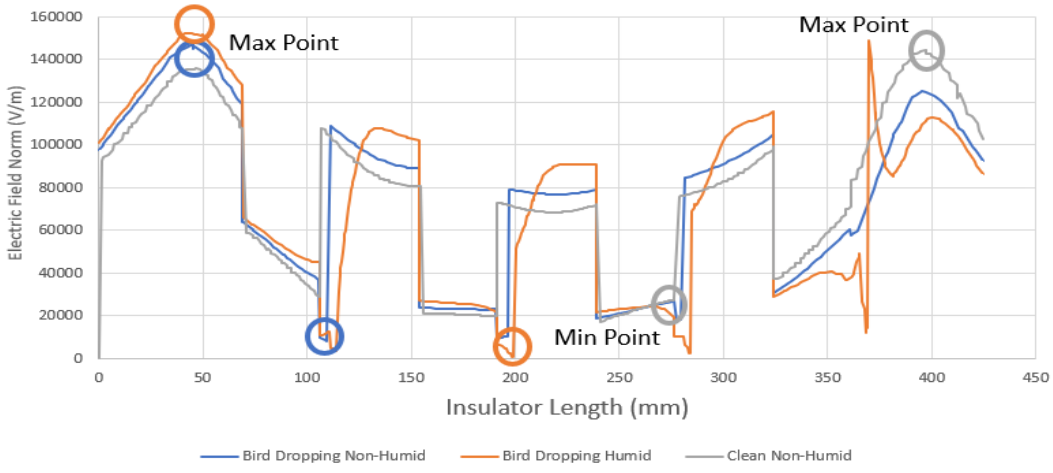

Figure 8: Electric field distribution in cross section 2D through a contaminated insulator (a) Bird Dropping Non-Humid (b) Bird Dropping Humid (c) Clean Non-Humid

3.3 Study of different levels of pollution layer thickness

Figure 9 illustrates the graph of the electric field distribution along the insulator for different thicknesses of bird-dropping contamination layers of 0mm, 5mm, and 15mm. From the graph, the bird-

dropping in humid gained the highest maximum electric field value with 152400 V/m. Then it was followed by bird-dropping in non-humid with 147150 V/m and clean insulator in non-humid with 144300 V/m. The values show that both bird-dropping with layers thickness of 5mm and 15mm have an increment percentage of difference maximum electric field by 1.97% and 5.12% compared with clean insulator with 0mm. The result indicates that as the thickness of the polluted layer increases, it creates a larger area with decreased dielectric strength. Thus, higher electric field intensifies concentrate in regions of lower dielectric strength, resulting in high electric field value.

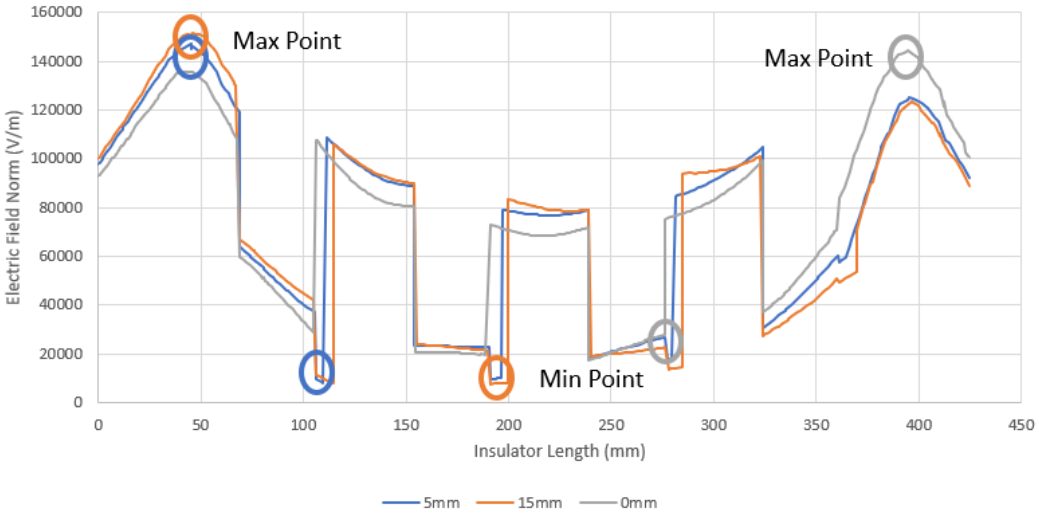

Figure 9: Electric field distribution in cross section 2D through a bird dropping insulator (a) 5 mm (b) 15 mm (c) 0 mm.

4. Conclusion

From the result obtained, the humid condition affects the performance of electric field distribution by a 3.53% increment compared with the non-humid condition. Secondly, the bird-dropping contaminant has the highest maximum electric field in non-humid conditions with 147150 V/m while the silica sand has the highest value in humid conditions with 253800 V/m compared to the others. This proves that different materials will have different changes in electric fields in certain conditions. Furthermore, the contaminated layer in humid and non-humid conditions shows a difference in maximum electric field by 5.62% and 1.97% compared with clean insulators in non-humid. This indicates the water droplets and contaminated layer affect the performance of the electric field. Finally, the level of thickness of 5 mm and 15 mm increased the electric field by 1.97% and 5.12% compared with clean insulators with 0 mm. The result proves that the electrical field increased as the contaminated layer increased.

Acknowledgement

The authors would like to thank the Faculty of Electrical and Electronic Engineering, Universiti Tun Hussein Onn Malaysia for its support.

References

[1] Hu, & Lu. (2017). Inspection and Monitoring Technologies of Transmission Lines with Remote Sensing. Inspection and Monitoring Technologies of Transmission Lines With Remote Sensing | ScienceDirect. retrieved November 5, 2022, from http://www.sciencedirect.com:5070/book/9780128126448/inspection-and-monitoring-technologies-of-transmission-lines-with-remote-sensing

[2] B. Hampton, “Flashover mechanism of polluted insulation”, *Proceedings of the Institution of Electrical Engineers*, , Vol. 111, (5): pp. 985-990, 1964

[3] Taherian. (2019). *Electrical Conductivity in Polymer-Based Composites*. Electrical Conductivity in Polymer-Based Composites | ScienceDirect. Retrieved November 5, 2022, from http://www.sciencedirect.com:5070/book/9780128125410/electrical-conductivity-in-polymer-based-composites

[4] A. C. Baker, M. Farzaneh, R. S. Gorur, S. M. Gubanski, R. J. Hill, G. G. Karady, and H. M. Schneider, "Insulator selection for AC overhead lines with respect to contamination", IEEE Trans. Power Del., Vol. 24, pp. 1633-1641, 2009.

[5] Murugan N, Sharmila G, Kannayeram G. Design optimization of high voltage composite insulator using electric field computations. In: 2013 International conference on circuits, power and computing technologies (ICCPCT). p. 315–20.

[6] *Reacon Electric Power Equipments Co.,Ltd*. (2023). Reaconelectric.com. http://reaconelectric.com/product_show.asp?cateid=46&ID=273

[7] R. de Jesus et al., “Hydrophobicity classification of distribution silicone arresters before and after solid layer contamination.”

[8] Liu, Y., Xinbo, H., Yang, H., & Liu, X. (2022, February 25). Simulation Study on Bird Droppings Flashover of Catenary Insulator Based on Finite Element Method. *2022 International Conference on Power Energy Systems and Applications (ICoPESA)*. https://doi.org/10.1109/icopesa54515.2022.9754466

[9] Braunger, M., Escanhoela, C., Fier, I., Walmsley, L., & Ziemath, E. (2012, October). Electrical conductivity of silicate glasses with tetravalent cations substituting Si. *Journal of Non-Crystalline Solids*, *358*(21), 2855–2861. https://doi.org/10.1016/j.jnoncrysol.2012.07.013

[10] *Relative Permittivity - the Dielectric Constant*. (n.d.). Relative Permittivity - the Dielectric Constant. https://www.engineeringtoolbox.com/relative-permittivity-d_1660.html

[11] Hussain, M. M., Farokhi, S., McMeekin, S. G., & Farzaneh, M. (2015, July). The effects of salt contamination deposition on HV insulators under environmental stresses. *2015 IEEE 11th International Conference on the Properties and Applications of Dielectric Materials (ICPADM)*. https://doi.org/10.1109/icpadm.2015.7295347

[12] Mohamed, I., Aramugam, K., & Khan, M. A. (2018, December). Simulation and Measurement of the Voltage Distribution on Porcelain Insulator String under Polluted Condition. *2018 IEEE 4th International Symposium in Robotics and Manufacturing Automation (ROMA)*. https://doi.org/10.1109/roma46407.2018.8986724